Mobility of Holes and Polarons in Polyaniline Thin Films Determined by Impedance Spectroscopy Measurements

R. Rutsch and J. Toušek

Charles University, Faculty of Mathematics and Physics, Department of Macromolecular Physics, Prague, Czech Republic.

Abstract. Impedance spectroscopy measurements were performed on polyaniline layers deposited on silicon substrates in the range of 110 Hz – 1 MHz. Different bias voltages were used during the experiment displaying regions of holes and polarons contributions to the mobility. The spectra had a character of space charge limited currents. Shift of the maximum of the spectra followed Poole–Frenkel law. Obtained results were compared with mobility estimated by CELIV measurements.

Introduction

Polyaniline (PANI) as a semiconductor with huge range of obtainable conductivities and easy synthesis is a convenient material for use in multiple branches throughout science and industry. Nowadays it is already used in various types of organic field effect transistors, gamma detectors or, in combination with silicon, in photovoltaic panels. Due to its conductive properties it can also be used e. g. in electrostatic discharge materials, conductive inks, chemical detectors (gas, toxic gas, bacteria or vitamin C sensor), OLED (organic light emitting diode) devices, membranes for gas separation etc. Detailed discussion of various applications and synthesis of PANI is in [1].

This polymer is known to have as a charge carriers holes, polarons and ions. The origin of the polarons in our layer was due to the protonation as it is shown in Figure 1. The protonation was done by introducing the layer to hydrochloric acid which reacted with an unpaired electrons on nitrogen atom of emeraldine base. This caused rearrangement of the electron bonds in quinonediimine ring to benzene ring and an unpaired electron on nitrogen atom called polaron was created. The polaron was partially delocalized along the backbone chain of the polymer and able to lead current.

For evaluation of the charge transport in semiconductor electronic devices mobility of charge carriers stands as an important parameter. In this study CELIV (charge extraction by linearly increasing voltage) method and impedance spectroscopy measurement were utilised to evaluate mobility of the charge carriers. The first mentioned method required injection of charge carriers by working electrodes or their generation by light pulse. The detailed description of the method is e. g. in [2]. For both methods we presumed that charge transport occurs in energy bands in protonated PANI salt as well as in emeraldine base. For impedance measurements we also presumed injection of holes and electrons from silicon wafer to PANI after application of negative charge to gold electrode (structure of the sample is shown in Figure 2a). Part of the injected charge forms polarons in the layer.

Other methods commonly used for evaluation of the charge carriers mobility are, e. g., time of flight, especially for thick layers, described in [3], electroluminescent transient methods that are applicable on light emitting diodes [4] or field effect transistor methods [5]. Last mentioned method has strong demands on geometry of the sample and brings little insight into the bulk properties.

Experimental part

Sample preparation

Thin PANI films deposited in silicon/glass/ITO-glass substrates were obtained from group led J. Stejskal from Institute of Macromolecular Chemistry AS CR. Layers were prepared as it is described in [6] utilising solution with 0.2 M concentration of aniline hydrochloride and 0.25 concentration of ammonium peroxidisulfate and protonated to conducting green PANI emeraldine salt with hydrochloric acid. Fraction of the samples were immersed in deionized water for 17 hour where PANI salt was converted to the base and then dried at 50 ºC for 15 min. in standard atmospheric conditions. Process of protonation and deprotonation of the sample is graphically described in Figure 1.

Measurements

Two series of PANI samples were under the investigation: PANI 2015 and PANI 2018.

The thickness of the layers was reported 60–160 nm by J. Stejskal group. Thickness of the water treated samples remained the same as it was revised by atomic force microscope (AFM) by J. Hanuš from the Department of Macromolecular Physics at Faculty of Mathematics and Physics of Charles University in Prague.

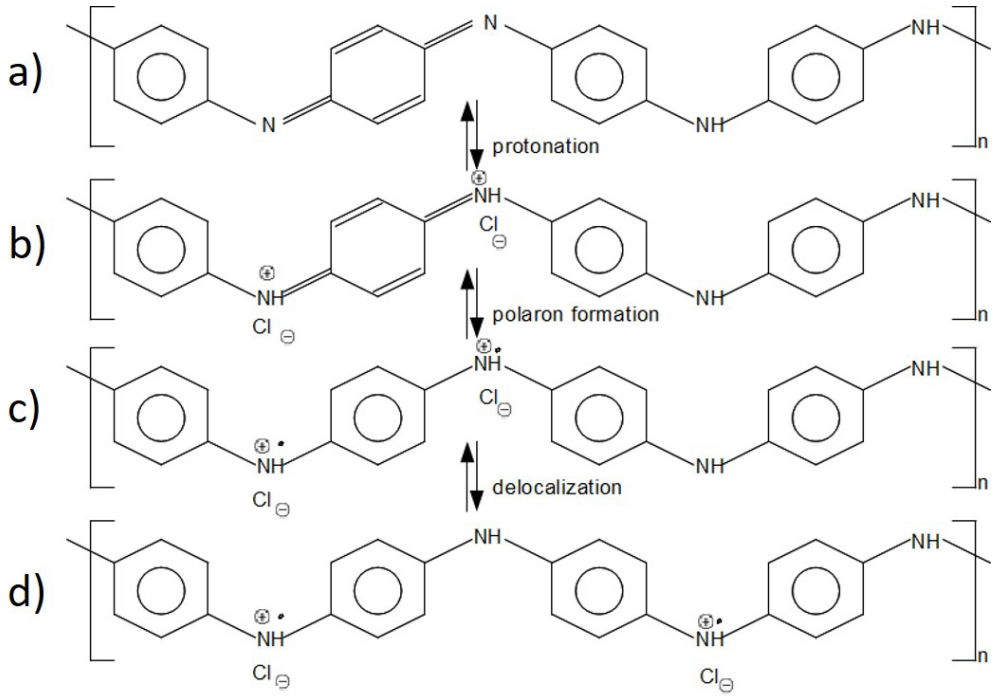

Figure 1. After the introduction of hydrochloric acid the double bond on the nitrogen of PANI base (a), atom is disrupted and electrons in quinonediimine ring are rearranged to form a benzene ring (b, c). The unpaired electrons on nitrogen creates polarons and PANI base is converted to PANI salt (c, d). Then polarons in PANI salt are able to move along the backbone of the polymer and are delocalised (d). Adapted and adjusted from [6].

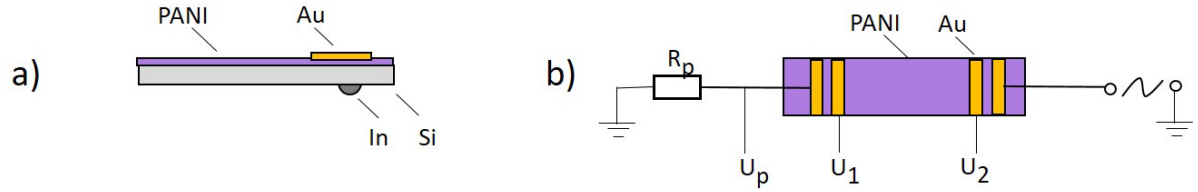

Figure 2. Composition of the measured samples with contacts. Part a) shows samples prepared on silicon substrates. By application of negative voltage to gold electrode, charge is injected from silicon wafer to the material. Part of the injected electrons create polarons. For the detailed energy band structure of the device see ref. [6]. Part b) illustrates composition of the sample on glass substrates used for conductivity measurements and simplified circuit composition. U_p represents voltage on element R_p with known resistivity, $U_1 - U_2$ represents voltage drop on specified sample area.

Gold contacts were deposited on the surface of both, water treated and as obtained, type of layers by evaporation under the low pressure of 2.7×10^{-3} Pa serving as p-PANI contact. An indium electrode was deposited on bottom side of Si wafer with solder to form n-Si contact. Resulting diode-like structure is depicted in Figure 2a.

The conductivity of the samples was measured by the system of parallel electrodes — two voltage and two current electrodes on layers deposited on glass substrates as it is shown in Figure 2b.

The impedance spectroscopy measurements were done in the dark at the room temperature covering the range from 110 Hz to 1 MHz. The amplitude for AC oscillation used for measurements was 0.1 V. Spectra at various DC voltages were measured. Agilent Precision LCR Meter E4980A was utilised to perform the experiment. The complex impedance was measured and for the purpose of analysation of charge carrier transport its imaginary part was used. Evaluation of imaginary part of the spectra was done under the presumption of polarons and holes captured in shallow traps, where energy barrier of the trap states acted as a capacity. This assumption led us to an equivalent circuit composed from capacity C parallel to resistivity R and equation:

$$Im(Z) = \frac{\omega C(U) R^2}{1+\omega^2 C^2(U) R^2}, \quad (1)$$

where ω represents applied frequency and capacity C is a function of applied DC bias voltages, where increasing DC voltage lowers the energy barrier of the trap states.

The measurements were performed in regime of non-stationary space charge limited currents, where injected charge (holes and polarons created from injected charge) from Si substrates was present. The injection of protons was blocked by the same electrodes and those carriers therefore did not contribute to the spectra. Under this conditions the mobility no longer depended on density of states in polymer and was dominated by injected charge:

$$\mu = \frac{d^2}{V\tau_{dc}}, \tag{2}$$

where τ_{dc} stands for transit time of charge carriers through the layer of thickness d. Numerical modification of transit time by factor 0.44 representing moderate dispersion of carriers were done according to [7] and [8]. Both, water treated and as obtained, samples were measured.

CELIV measurements were taken on apparatus consisted from OWON Smart DS 7102V digital oscilloscope, a functional generator Agilent 333250A and a sample holder constructed in lab. The whole experiment was performed in dark at the room temperature and normal atmospheric surrounding. The structure of the sample was as it is described in Figure 2a. Gold electrode functioned as ohmic contact to PANI and indium works to the same purpose for Si wafer. We applied saw-shaped pulse to the gold contact. For injection of charge carriers negative offset of the applied pulse was utilised. The dielectric relaxation time is considered several orders of magnitude faster than transit time resulting in distribution of the charge into the whole volume of the layer. At the positive part of the pulse charge carriers were being extracted. The current response of the device in time was recorded by oscilloscope. Modulation of the current response with respect to the applied pulse determined the mobility. We presumed that majority of injected charge were holes, because injection of the electrons from Si to PANI is blocked by energy barrier of 2.6 eV on the junction of materials while the same contact held little resistance for holes. The detailed energy structure of the junctions is depicted in ref. [6].

Results and discussion

The measured series of negative imaginary impedance are shown in Figures 3 and 4 for protonated samples and water treated sample respectively. Used DC voltages were in range from –0.5 V to –5 V for PANI 2018

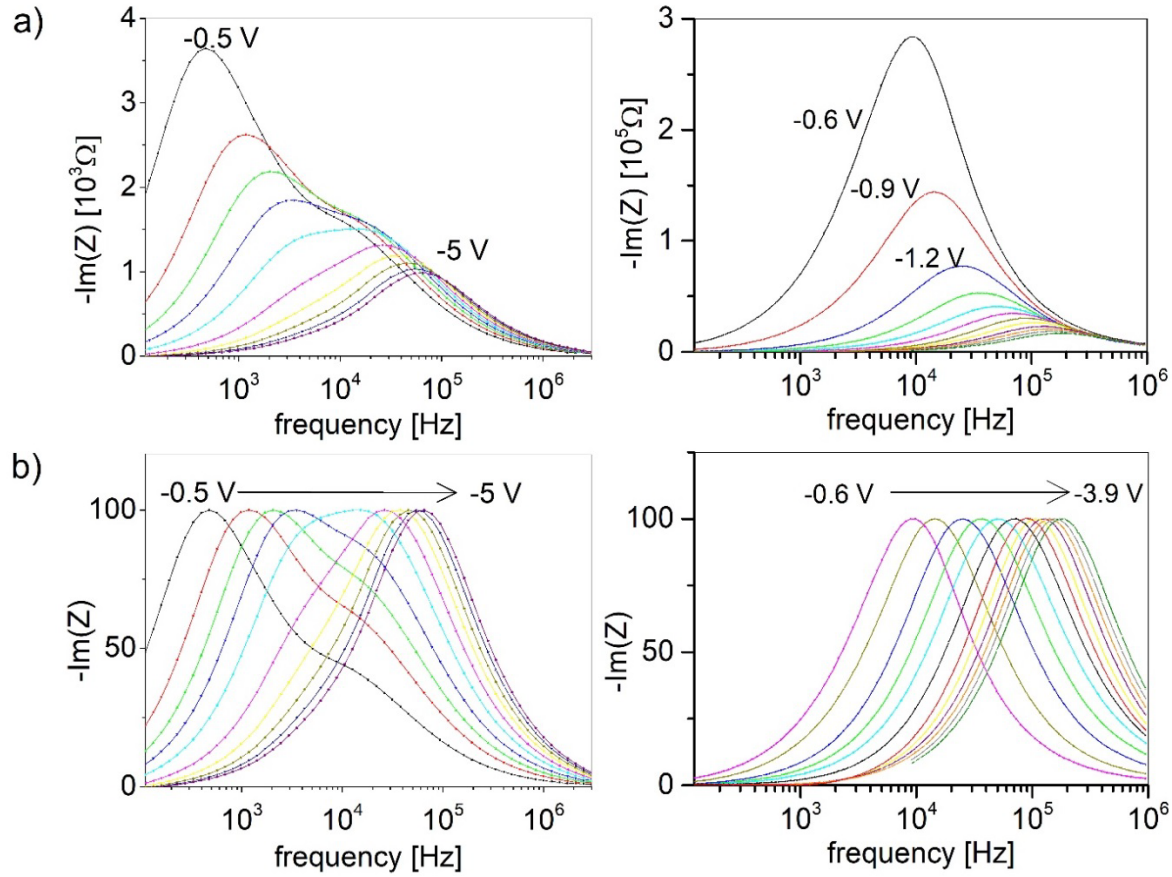

Figure 3. Impedance spectra measured on PANI 2018 (on the left) and PANI 2015 (on the right) evaluated for negative imaginary part. Measurements of protonated samples is depicted. Part a) shows measured amplitudes, part b) shows rescaled spectra.

samples and from –0.6 V to –4 V for PANI 2015 samples. Resistance of the contacts prevented us from usage of lower bias voltages. With increasing DC voltages portion of the trapped charges was released and no longer contributed to the characteristic. This explains decrease in amplitude for non-rescaled spectra in Figures 3a and 4a. For better illustration of the change in spectra, those were rescaled (Figures 3b and 4b) using value 100 as the maximum.

From equation (1) the condition for the maximum of the spectra is given as: $\omega RC(U) = 1$. Applied bias voltage lowered energy barrier of the trap states which together with condition mentioned above explains shift of the maximum of the spectra with increasing DC voltages to the higher frequencies.

In Figure 3 we observed two groups of peaks that are clearly distinguishable especially in PANI 2018 samples. The group with lower frequency peaks was assigned to heavier polarons. Their intensity in the spectra is high and shields the visibility of holes contribution in the low frequency region. From the resulting spectra we assumed polaron trap states being more shallow than hole trap states as this contributions disappeared completely at around 2.5 V DC bias. Above this voltage all polarons were assumed to be released from trap states. In water treated sample in Figure 4 the contribution of polarons did not appear in agreement with deprotonation process assumed as it is depicted in Figure 1.

The second group of peaks in Figure 3 for higher frequencies was assigned to lighter holes. Their contribution were observable up to 4–5 V of negative bias voltage. After that all charge carriers were detrapped and characteristic was no longer obtainable. The impedance characteristic was presumed to depend on the density of trapped occupied states interacting with the alternating current. Water treated samples showed little change for high frequency peaks which is in accordance with the assumptions.

The peak for lower frequencies than both polarons and holes contributions that appeared for lowest DC voltage in Figure 4 was assumed to be caused by remained water vapours in polymer layer after the water treatment.

Mobility of the charge carriers

According to [7] the peak in impedance spectra represents the transit time of charge carriers. The mobility of the samples was estimated according equation (2) with numerical factor $\tau_{dc} = 0.44\tau_{peak}$ representing moderate dispersion [8, 9]. Obtained values were plotted against the square root of the applied electric field $E^{1/2}$ in logarithmic scale and are depicted in Figure 5. Linearity of the characteristic indicates Poole–Frankel mechanism and confirms the existence of the traps in the material:

$$\mu = \mu_0 \exp\left(\beta\sqrt{E}\right). \tag{3}$$

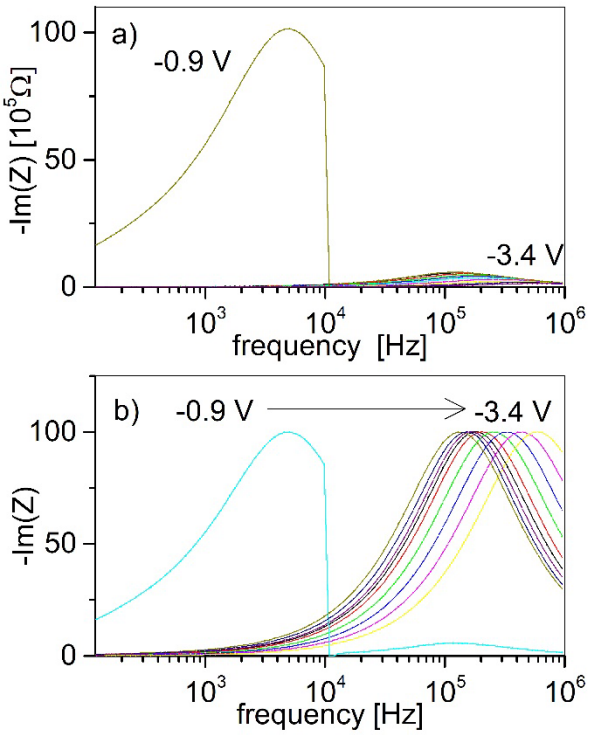

Figure 4. Impedance spectra measured on PANI 2015 evaluated for negative imaginary part. Measurements of water treated samples is depicted, a) shows measured amplitude and b) shows rescaled spectra.

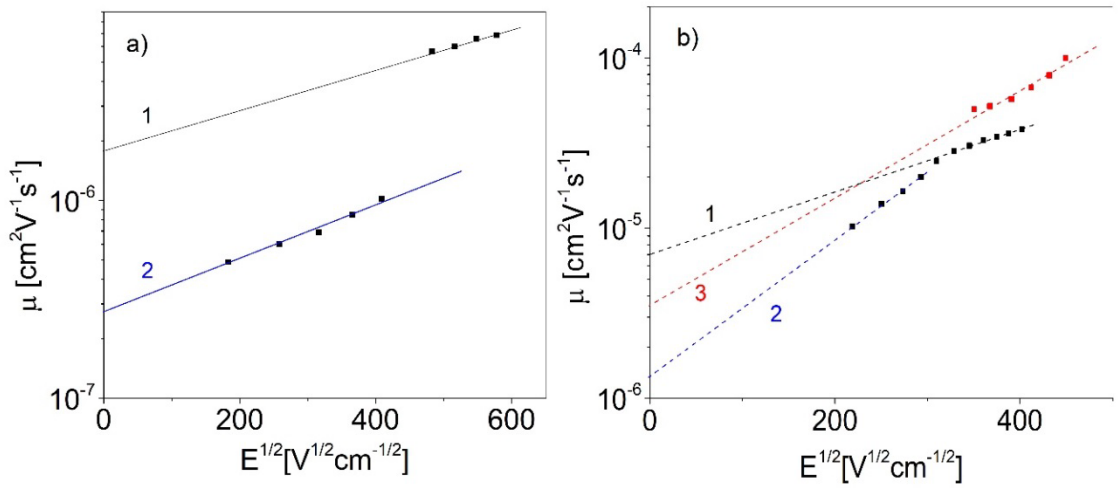

Figure 5. Mobility plot assuming Poole–Frankel mechanism a) for PANI 2018 and b) for PANI 2015. Curves 1a) and 1b) (black) represents linear fits for holes in protonated sample, curves 2a) and 2b) (blue) shows behaviour of mobility for polarons in protonated samples and red curve 3b) represents mobility of holes in water treated sample.

The resulting mobilities of examined samples were $\mu_{02018} = 1.8 \times 10^{-6}$ cm^{2}V^{-1}s^{-1} and $\mu_{02015} = 6.9 \times 10^{-6}$ cm^{2}V^{-1}s^{-1} for holes in protonated sample and $\mu_{02018} = 2.7 \times 10^{-7}$ cm^{2}V^{-1}s^{-1} and $\mu_{02015} = 1.4 \times 10^{-6}$ cm^{2}V^{-1}s^{-1} for polarons in protonated sample. Mobility of holes in water treated sample were $\mu_{02015} = 4.0 \times 10^{-6}$ cm^{2}V^{-1}s^{-1}. For comparison of results of both methods, values $\mu_{2018} = 3.7 \times 10^{-6}$ cm^{2}V^{-1}s^{-1} and $\mu_{2015} = 2.7 \times 10^{-5}$ cm^{2}V^{-1}s^{-1} at the field 1.0×10^5 Vcm^{-1} for holes in protonated samples were calculated at equivalent field in the CELIV measurements.

Mobility of PANI 2015 samples was also estimated by CELIV method. There we used frequencies around 1 MHz. Utilised electrodes were blocking for the ions. As it is shown in previous section, polaron characteristic was visible in lower frequency range, therefore we attributed measured mobility to the holes. The calculations were performed according to the equation in ref. [9]:

$$\mu = \frac{2d^2}{3A(t_{max}-t_0)^2}\left(\frac{1}{1+0.36\frac{\Delta j}{j(0)}}\right), \tag{4}$$

where d stands for thickness of the layer, $j(0)$ is the capacitive displacement current, A represents slope of the pulse, Δj peak is current diminished by $j(0)$ at the time t_{max}.

The obtained characteristic is shown in Figure 6 and estimated average value of mobility from multiple measurements is $\mu_{2015} = 2.4 \times 10^{-5}$ cm^{2}V^{-1}s^{-1} at the field 1.0×10^5 Vcm^{-1}.

Conductivity of the layer

The conductivity of PANI layer was measured utilising parallel gold current and voltage electrodes as it is illustrated in Figure 2b. The results are shown in Table 1. This measurement does not distinguish the type of the charge carrier and the measured value represents the combined conductivity of all three types of carriers included in samples (holes, polarons and ions).

Table 1. Conductivities of the samples.

sample	Conductivity of protonated sample	Conductivity of water treated sample
PANI 2015	5 Scm^{-1}	2.2×10^{-5} Scm^{-1}
PANI 2018	3.5 Scm^{-1}	2.5×10^{-5} Scm^{-1}

The value of HOMO 5.1 eV was estimated by Stejskal group by cyclic voltammetry. The work function was estimated by Kelvin probe method as it is shown in ref. [10]. Then, the concentration of holes was calculated from the equation:

$$p = N_v exp\left(-\frac{E_F - E_{HOMO}}{kT}\right), \tag{5}$$

where effective density $N_v = 8.8 \times 10^{21}$ cm^{-3} was estimated under the conclusion that each monomer unit contribute with one state and the density of PANI is 1.33 gcm^{-3} resulting in value: $p = 2.9 \times 10^{18}$ cm^{-3}.

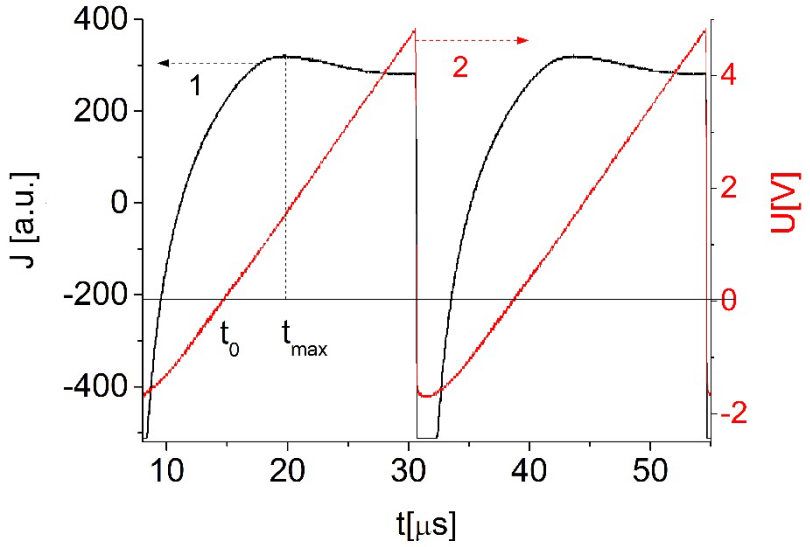

Figure 6. Dark CELIV current characteristic (black curve) and applied pulse (red curve).

From known conductivity equation, $\sigma = pe\mu$, using estimated concentration and mobility of holes determined from both CELIV and impedance spectroscopy method for protonated sample PANI 2015, we determined the conductivity caused by holes $\approx 1 \times 10^{-5}$ Scm^{-1}. This value is significantly lower than conductivity estimated by direct measurement of protonated sample. From this fact we assumed that the conductivity of the protonated sample is mainly driven by ions with very small contributions of other carriers. The conductivity directly measured on water treated samples was higher but in the same magnitude as calculated value. This can point out that deprotonation of the sample was not done by 100% and tiny amount of protons and polarons remained in the layer. In situ prepared PANI on silicon substrates are known to show anisotropic behaviour and conductivity of the layer tends to be higher in direction of the growth which is identical with direction of CELIV and impedance measurements. For direct measurement of conductivity of the protonated sample in direction of growth of the layer very fine geometrical condition would be necessary. Based on the possible anisotropy of the material we can presume that the directly measured conductivity would be even higher than conductivity measured with four electrode system.

Conclusion

Two methods for evaluation of the mobility of charge carriers in PANI films were used. Both method used the same configuration (Figure 2a) and excluded contributions of ions in measured data. Impedance spectroscopy performed in the range 110 Hz – 1 MHz for various DC voltages yielded two groups of peaks. The lower frequency contributions were assigned to polarons and disappeared from spectra after deprotonation of the layer by water treatment. The second group at higher frequencies was not influenced by water treatment and it was assigned to holes. The resulting mobilities according to equation (2) were plotted against square root of electric field giving linear slopes for respective contributions and confirming Poole–Frenkel mechanism of releasing the charges from the traps. The mobility evaluated from slope of the mentioned plot $\mu_{2015} = 2.7 \times 10^{-5}$ cm^{2}V^{-1}s^{-1} at the field 1×10^5 Vcm^{-1} was compared with the average value obtained by CELIV measurements $\mu_{2015} = 2.4 \times 10^{-5}$ cm^{2}V^{-1}s^{-1}. Both values are in good agreement.

Conductivity directly measured on the samples deposited on glass substrates was 5 Scm^{-1} which was several orders of magnitude higher than conductivity of holes calculated with respect to HOMO level and work function that gave as value 1×10^{-5} Scm^{-1}, indicating domination of ions in conductivity of the protonated samples.

Acknowledgements. The authors thank the Stejskal group for deposition of PANI samples, and Dr. Hanuš for AFM measurements.

References

[1] Bhadra, S., D. Khastgir, N. K. Singha, J. H. Lee, Progress in preparation, processing and applications of polyaniline, Progress in Polymer Science, 34, 783–810, 2009.

[2] Juška, G., K. Arlauskas, M. Viliunas, J. Kocka, Extraction Current Transients: New method of Study of Charge Transport in Microcrystalline Silicon, Phys. Rev. Lett., 84, 4946–4949, 2000.

[3] Choulis, S. A., J. Nelson, Y. Kim, D. Poplavskyy, T. Kreouzis, J. R. Durrant, D. D. C. Bradley, Investigation of transport properties in polymer/fullerene blends using time-of-flight photocurrent measurements, Appl. Phys. Lett., 83, 3812, 2003.
[4] Karl, N., Charge carrier transport in organic semiconductors, Synthetic Metals, 134, 649–657, 2003.
[5] Geens, W., T. Martens, J. Poortmans, T. Aernouts, J. Manca, L. Lutsen, P. Heremans, G. Borghs, R. Martens, D. J. Vanderzande, Modelling the short-circuit of polymer bulk heterojunction solar cells, Thin Solid Films, 452, 498–502, 2004.
[6] Toušek, J., J. Toušková, R. Chomutová (Rutsch), I. Křivka, M. Hajná, J. Stejskal, Mobility of holes and polarons in polyaniline film assessed by frequency dependent impedance and charge extraction by linearly increasing voltage, Synthetic Metals, 234, 161–165, 2017.
[7] Tripathi, C. D., A. K. Tripathi, Y. N. Mohapatra, Mobility determination using frequency dependence of imaginary part if impedance (Im Z) for organic and polymeric thin films, Appl. Phys. Lett., 98. 033304, 2011.
[8] Boudiba, S., A. Růžička, C. Ulbricht, S. Enengl, C. Enengl, J. Gasiorovsky, Polymers with Alternating Anthracene and Phenylene Building Blocks Linked by Ethynylene and/or Vinylene Units: Studying Structure Properties Relationship, Journal of Polymer Science, 55, 129–143, 2017.
[9] Juška, G., K. Arlauskas, M. Viliūnas, K. Genevičius, R. Österbacka, H. Stubb, Charge transport in π-conjugated polymers from extraction current transients, Phys. Rev., B62, R16235, 2000.
[10] Toušek, J., J. Toušková, Z. Remeš, R. Chomutová, J. Čermák, M. Helgesen, J. E. Carlé, F. C. Krebs, Electrical characterization of fluorinated benzothiadiazole based conjugated copolymer — a promising material for high-performance solar cells, AIP Advances, 5, 127240, 2015.